The impact of accumulation rate on anisotropy and air permeability of polar firn at a high-accumulation site

Maria W. HÖRHOLD,[1] Mary R. ALBERT,[2] Johannes FREITAG[1]

[1]*Alfred Wegener Institute for Polar and Marine Research, Am Handelshafen 12, D-27570 Bremerhaven, Germany*
E-mail: Maria.Hoerhold@awi.de
[2]*US Army Cold Regions Research and Engineering Laboratory, 72 Lyme Road, Hanover, New Hampshire 03755-1290, USA*

ABSTRACT. The first three-dimensional properties of polar firn obtained by X-ray microtomography are used to study the microstructure of snow on a 15 m deep firn core from West Antarctica. The snow is found to undergo coarsening down to approximately 2.5 m depth before grain growth and densification become the prevalent mechanisms of microstructure change. In contrast to previous assumptions, distinct anisotropy of the ice and pore geometry is observed throughout the profile, with a maximum at 2.5 m depth. The air permeability and the degree of anisotropy vary with depth and can be linked to short-term changes in accumulation rate via the residence time for which a certain snow layer stays in the uppermost 2.5 m. Patterns of the degree of anisotropy and air permeability of buried polar firn are relative indicators of past accumulation rates.

INTRODUCTION

On polar ice sheets the surface snow and firn forms a layered and porous medium that remains permeable to gases over depths of many tens of meters. Local surface conditions affect the generation and transformation of the snow and firn column; the temperature by affecting the rate of densification, and the accumulation rate by forming the layering and determining the time the snow is exposed to insolation and temperature gradients at the surface. Single snow layers are created by depositional events and consist of very different snow types, leaving a highly stratified firn pack (Gow, 1965; Alley and others, 1982; Palais and others, 1982; Alley, 1988). Since the properties of the different snow layers are very distinct in grain and pore size, forming diverse stratigraphic horizons (Palais and others, 1982), they transform differently in applied temperature gradients and load (Alley and others, 1982).

The microstructure of surface snow and the stratigraphic and grain-scale characteristics vary spatially with varying accumulation rates on the East Antarctic ice sheet (Watanabe, 1978; Shiraiwa and others, 1996), as does the air permeability (Courville and others, 2007). However, it is not clear how short-term changes in temperature or accumulation rate are reflected in the firn properties over time, as subsequent burial moves layers down through the firn column. For a relatively high-accumulation site in West Antarctica, Rick and Albert (2004) discuss the impact of temperature and accumulation rate, on seasonal and decadal scales, on the permeability and microstructure of firn. Albert and others (2004) report that low accumulation rates, in areas like the East Antarctic plateau, cause extreme firn metamorphism, due to the length of time the snow is exposed to insolation and wind at the surface. Small differences in accumulation rate create very large differences in microstructure, permeability and thermal conductivity in the top meters of firn, which leave an enduring record as the firn becomes buried (Rick and Albert, 2004; Courville and others, 2007). The occurrence of highly permeable and porous layers at greater depths in the megadunes area documents that a change in climate conditions would influence both the microstructure and the permeability. At least at cold, low-accumulation sites, a signature of changing accumulation rate is maintained in the microstructure and air permeability of the firn column.

Earlier studies addressing polar snow microstructure used thin or thick sections from firn samples to obtain information about the microstructure (Gow, 1969; Alley and others, 1982; Rick and Albert, 2004). This technique enabled only a two-dimensional analysis, and the quantitative microscopy is limited (Davis and others, 1996). Recently, X-ray microtomography has been used to study alpine or artificial, sampled or sieved snow, observed for different time intervals in the laboratory (Flin and others, 2004; Schneebeli and Sokratov, 2004; Kaempfer and others, 2005; Kaempfer and Schneebeli, 2007). In experimental set-ups for isothermal metamorphism (Flin and others, 2004; Kaempfer and Schneebeli, 2007), temperature gradient metamorphism (Schneebeli and Sokratov, 2004) and micromechanical studies (Pieritz and others, 2004), it has been shown that snow can be correctly described using microtomography and image-analysis tools (Coléou and others, 2001).

In this study, for the first time, microtomography is used to profile polar firn with varying layers and properties. A 15 m long firn core drilled during the US ITASE (International Trans-Antarctic Scientific Expedition) campaign 2002 at Hercules Dome is used to investigate the snow and firn microstructure and air permeability. Hercules Dome is situated at 86° S, 105° W, with relatively high accumulation rates of 0.16–0.20 m w.e. a^{-1} over the last 300 years and low temperatures of –35 to –40°C (Jacobel and others, 2005). Permeability measurements and microtomography are used to describe the evolution of the microstructure with time and depth. We observe a stratigraphically induced high variability in microstructure and air permeability and a distinct anisotropy of the firn throughout the profile. In addition, influences that induce variations of the firn characteristics over a longer-term trend (and hence, across multiple layers) impact the anisotropy and air-permeability profile. These longer-term variations are superposed on the layering and the changes that occur with depth due simply to layer deposition, densification and other processes. By considering

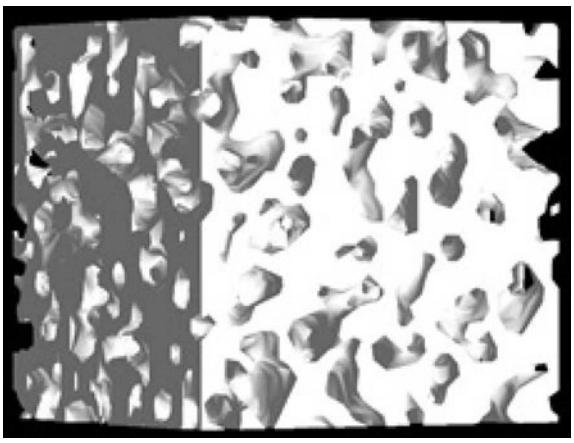

Fig. 1. A reconstructed firn cube with side length 16 mm showing the pore phase from 2.5 m depth. White is the pore phase; voids represent the ice grains.

the time the snow is exposed to near-surface conditions, we can link these variations to short-term changes in the accumulation rate. Our results confirm that changes in accumulation rate leave a signature in the firn permeability and microstructure as the firn becomes buried.

METHODS

The firn-core permeability was measured following the procedures described by Albert and others (2000), Rick and Albert (2004) and Courville (2007). The measurements were applied at 220 homogeneous firn-core sections, as identified on a light-table, of 3–10 cm length. Due to poor core quality, no permeability data were available in several intervals of the uppermost 2 m and at 8.5–9.5 m depth. Homogeneous coarse-, fine- and medium-grained layers, distinguished by visual inspection of the grain size relative to the surrounding layers, were sampled in every depth interval of the firn core for further analysis. Microstructural properties of the firn grain and pore space were obtained at –25°C by X-ray microtomography using a micro-CT (computed tomography) scanner (1074 SkyScan) inside a cold room. A charge-coupled device (CCD) camera of 768×512 pixels and 256 grey levels was used as an X-ray detector. Cylindrical snow and firn samples of 2 cm diameter and height were drilled out of the main core with a hole saw. The sample was placed on a turntable in front of the source, and was rotated in 0.9° intervals during scanning. A set of 210 shadow images was captured while the rotation completed a semicircle.

A convolution algorithm with a back projection for fan beams transformed the shadow images into a series of horizontal cross-sections representing the three-dimensional (3-D) structure of the snow. The resolution as well as the distance between adjacent reconstructed images was 40 μm, so the object was displayed by a 3-D grid of grey image values (voxels) with a spacing of 40 μm in the x, y and z directions. For digital image analysis a cubic region of 16 mm side length (leaving $400 \times 400 \times 400$ voxels) was chosen out of the cylindrical sample. A sample 3-D image is shown in Figure 1. The image size is large enough to sufficiently represent the firn properties (Hörhold, 2006; Freitag and others, 2008).

The image-processing and analysis procedures were conducted with *MAVI* (Modular Algorithm for Volume Images), a software for analyzing 3-D material, developed by the Fraunhofer Institute (Armbrecht and Sych, 2005). After application of filter and segmentation procedures, an additional object filter was used to remove all objects adding less than 1% to the total pore or ice volume.

All parameters were obtained and analyzed referring to the volume of the firn cube. The porosity of a sample is given by the ratio of void representing voxels to the total voxel number of the firn cube. A measure for grain and pore size is the grain- and pore-chord length, defined as the mean intersection of a line with the object being the void or the grain in different directions (Ohser and Mücklich, 2000). The measurement of the surface area and the integral of mean curvature is based on the application of the so-called Crofton's intersection formulae (Ohser and Mücklich, 2000; Armbrecht and Sych, 2005). The surface density represents the ratio of the ice–air surface and the corresponding volume of the ice phase. Small-grained snow from the near surface will have a larger surface density than sintered, well-rounded snow deeper down the firn column. The integral of mean curvature is defined as the mean of the minimum and maximum curvature at each surface element, integrated over the whole surface of the volume (Ohser and Mücklich, 2000). It therefore is a measure of the curvature of the ice phase's structure and displays the size and roundness of the ice matrix. Divided by the number of voxels of each sample, we obtain a mean value for the sample, so negative values represent a mean of concave forms, and positive values a mean of convex forms within the firn cube. Dendritic crystals will show negative values and large, smooth surfaces result in curvature values around zero.

The strength of *MAVI* is that it enables the 3-D study of structure characteristics related to the surface density. Each surface element of a microstructural component can be represented by a surface-normal vector with its specific direction. The surface-normal distribution displays the directional distribution of all surface-normal vectors. Apart from gravitational settling along the z axis in the snow, vertical temperature gradients result in vertical water-vapor transport within the snowpack. Thus a preferential direction of the texture is to be expected in the vertical direction, and isotropic behaviour in the horizontal direction. Therefore in this paper we study the fraction of surface-normal vectors orientated in two horizontal and the vertical directions with an apex angle of 30° (Armbrecht and Sych, 2005). We take the ratio of the fractions of the horizontal directions (the mean of the two horizontal fractions) and the vertical direction (s-n fraction). The ratio for an istotropic texture such as a sphere will be 1, whereas the ratio of a texture elongated within the horizontal plane will be >1, and a texture elongated in the vertical plane will be <1 (Ohser and Mücklich, 2000).

Depending on the length of the core pieces (3–10 cm, as designated on the light-table), two to five subsamples were analyzed by micro-CT and averaged, representing the microstructure of that specific layer. In order to study larger-scale features, a running mean was applied with a window length covering several layers and weighting the points by the number of measured subsamples.

Density measurements within the uppermost 2.5 m of firn were used to convert this to a water equivalent depth of 0.9 m. Measured accumulation rates (personal communication from D. Dixon, 2006) were then used to calculate the time taken for a snow layer to be buried to a depth of 2.5 m.

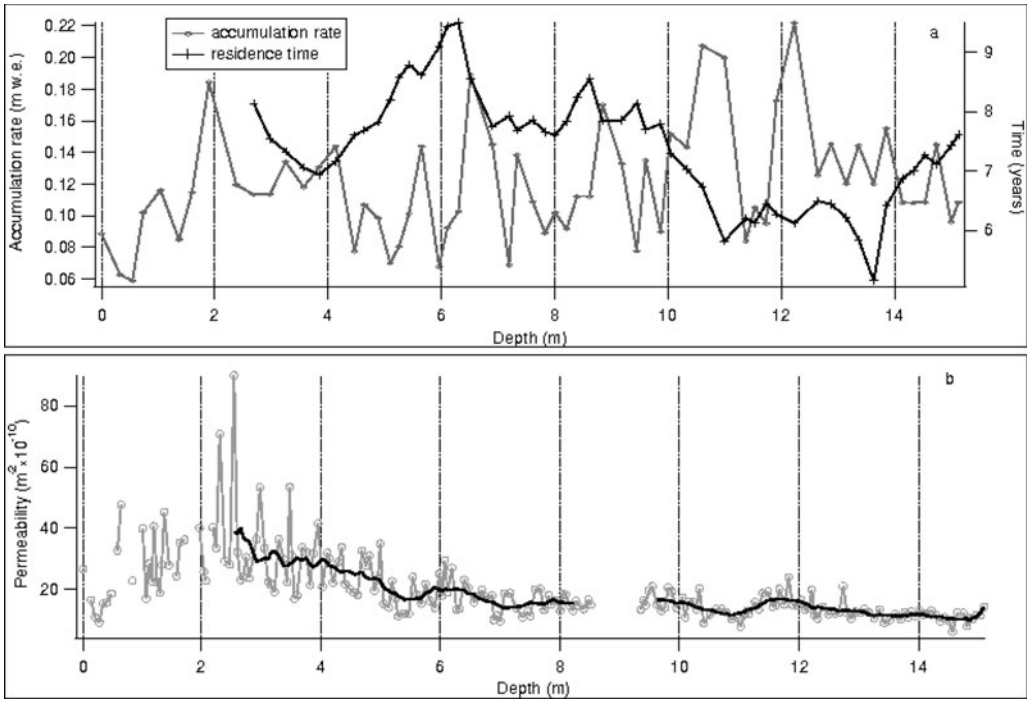

Fig. 2. (a) The accumulation rate as obtained by chemical analysis together with the calculated residence time in the uppermost 2.5 m and (b) the measured air permeability. The black curve is the running mean average over the different layers, starting from 2.5 m.

RESULTS

At Hercules Dome for the most recent 60 year accumulation estimates, based on chemical analysis and density measurements, a mean accumulation rate of approximately 0.12 m w.e. a^{-1} is observed (Fig. 2a). The calculated residence time within the uppermost 2.5 m shows a peak near 6 m depth, a local minimum below, a second peak near 8.5 m depth, and then generally decreases, with a local maximum near 12 m depth (Fig. 2a).

The results for permeability are shown in Figure 2b, and microstructural characteristics are shown in Figure 3. We observe a large variability of all parameters due to the layering of the firn. For the chord length in grain size and pore space (Fig. 3a and b) we find clearly larger values for the vertical than for the two horizontal directions. The ratio of the normal vector fractions is plotted in Figure 3f. A ratio of 1 indicates isotropy. Values less than 1, as found here, show that more surface-normal vectors point in the horizontal plane than in the vertical plane. The firn texture is vertically anisotropic.

In order to display the long-term trend, the running mean is calculated for all parameters (Figs 2b and 3). For the permeability we find an increase until 2.5 m depth. The permeability below is decreasing, but shows two local maxima near 6 and 12 m depth (Fig. 2b). Both the grain size and the pore size increase rapidly until 2–3 m depth. Below, the pore size decreases slowly (Fig. 3a and b). Whereas the porosity almost linearly decreases with depth (Fig. 3c), surface density and the mean of the integral of mean curvature rapidly decrease and increase respectively until 2 m depth, continuing their trend, but at more gradual rates, below this (Fig. 3d and e). For the anisotropy we find an increase until 2–3 m depth, and then a decrease, but with a region of low anisotropy between 7 and 8 m depth followed by a region of increased anisotropy near 10 m depth (Fig. 3f).

The increase in the chord lengths and the mean of the integral of mean curvature and the decrease of surface density imply coarsening of the texture until 2–3 m depth, accompanied not only by maximum permeability and pore size but also by maximum anisotropy. Here we refer to coarsening of firn as a general increase in both the grain size and the pore size. Below that, densification becomes significant, and continued gradual metamorphism decreases pore size and porosity while continuously increasing the grain size. At this site the firn is highly stratified, with each layer showing very different properties in terms of microstructure, permeability and development of anisotropy. The illustrated variation in the longer-term trends, particularly in the permeability and anisotropy profiles, is not related to the layering but to longer-term processes.

ANISOTROPY

At Hercules Dome the maximum degree of anisotropy is reached at approximately 2.5 m depth (Fig. 3d). However, in contrast to previous studies (Alley, 1987), we find that anisotropy does exist below that, though it tends to decrease with depth. Moreover, these data show that anisotropy does not decrease in monotonic fashion, but rather that there are depths at which anisotropy is strongly pronounced and other depths at which it is not.

Yosida and others (1955) and Colbeck (1983) introduced models of oriented crystal growth. In natural snow subjected to changes in weather, temperature gradients are mostly oriented in the vertical direction. The temperature gradients then induce gradients in water-vapor transport. Crystals grow by condensation of water vapor on their bottom portions, because the bottom of a growing particle is cold relative to the average snow temperature at its height (Colbeck, 1983). Alley and others (1982) found that crystals in coarse firn exhibit a strong vertical shape orientation near the surface, which can be attributed to the strong vertical water-vapor and heat transport.

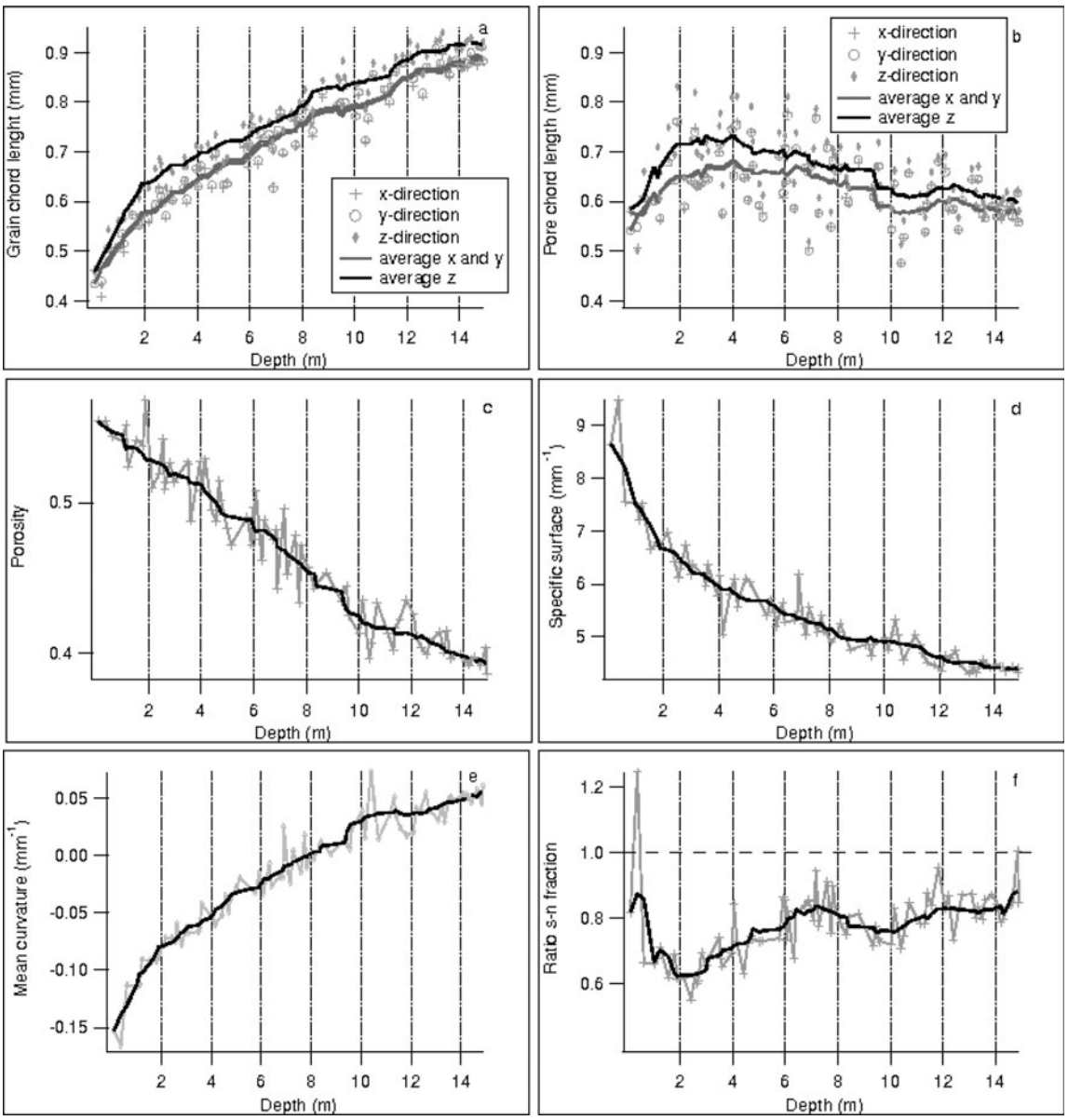

Fig. 3. (a, b) The mean grain (a) and pore (b) chord lengths in *x*, *y* and *z* directions. Dark curves represent the running mean (grey for horizontal; black for vertical). (c–f) The porosity (c), surface density (d), mean curvature (e) and ratio of the normal vector fractions s-n (f),

On the other hand, Schneebeli and Sokratov (2004) found in temperature gradient experiments with different snow layers that anisotropy occurred in dense, fine-grained layers, whereas low-density layers exposed to similar gradients did not show an anisotropy texture after the same time interval. Our data support these observations: we find highly porous layers to be less anisotropic than less porous layers in the same depth interval. The small-scale variability in the anisotropy profile is probably controlled by the different formation of anisotropy in the different layers.

ACCUMULATION RATE AND RESIDENCE TIME

From the microstructure and permeability data we can conclude that despite the very different properties of the different layers in terms of permeability and anisotropy, the larger-scale features shape the evolution with depth. These features are visible in both the low- and high-permeability layers and in the low- and high anisotropy layers respectively. The observed variability does not originate from the layering nor the linear compaction with depth. Changes in the metamorphic regime must be the basic cause. A major parameter determining the metamorphism is the impact of the accumulation rate, which, however, is difficult to parameterize since it superimposes the effects of the layering and densification.

The maximum in coarsening, permeability and anisotropy is obtained by 2.5 m depth, while below that, densification combined with slow grain growth appears to become important. It appears that, at this site, as long as a certain layer stays in the uppermost 2.5 m, it is exposed to significant temperature gradients, periodically higher annual temperatures and metamorphically induced coarsening. We hypothesize that the degree of coarsening, permeability and anisotropy of each layer deeper down the firn column is designated by the degree of these parameters at 2.5 m depth. In turn the degree at 2.5 m depth results from the history between 0 and 2.5 m depth, i.e. the time spent in the near-surface area. This residence time depends only on the accumulation rate.

We test the possibility that the time that snow spends in the near surface influences its permeability and anisotropy at

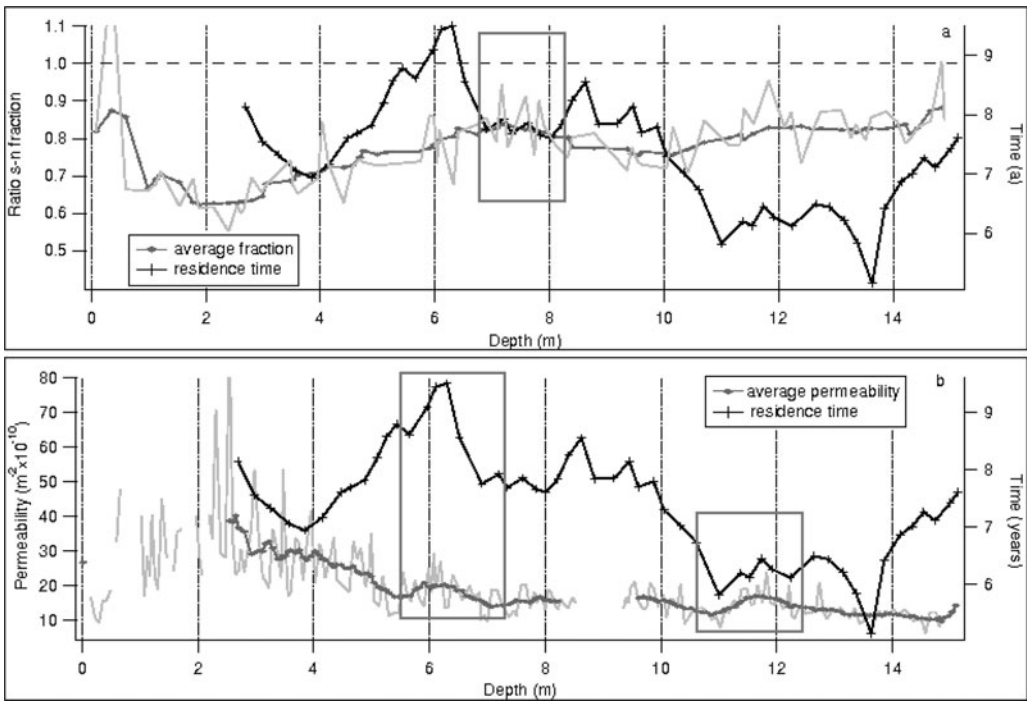

Fig. 4. The residence time with mean anisotropy (a) and air permeability (b).

depth, by using the density to calculate residence time in the near surface (Fig. 2a). Since the accumulation rate and thus the residence time were calculated on different scales and samples than the microstructure and permeability, here we can only compare the evolution with depth of these two different parameter sets (Fig. 4a and b).

An examination of the residence time in comparison with the average anisotropy in Figure 4a shows that it is the zone between 7 and 8 m where the surrounding long residence times are briefly interrupted by a phase of decreased residence time. When the firn at 7–8 m depth in this firn core was near-surface snow, it did indeed spend less time in the near surface. The shorter time that it spent in the near-surface region of higher temperature gradients means that it was less exposed to rapid metamorphic processes. The result is that the firn structure at 7–8 m shows low vertical anisotropy (Fig. 4a). As shown in Figure 4a, the residence time in the near-surface area decreases below 10 m depth and thus results in a less anisotropic character. The features of very short residence time around 11 m and at 13–14 m are not reflected in anisotropy.

In Figure 4b the measured air permeability is shown, together with the residence time. The peak in permeability at 2.5 m depth is due to the maximum of coarsening. Similar increases in permeability down to 2–4 m have been reported previously at different high-accumulation polar sites (Albert and others, 2000; Albert and Schulz, 2002; Rick and Albert, 2004). The second maximum around 6 m depth and at 11–12 m can again be linked to the residence time. Increased residence time strengthens the connectivity of the pore space and by that the air permeability of the firn. The residence-time minima at 7 and 11 m coincide with distinct permeability minima. Nevertheless there are areas where a correlation is not apparent, such as the decrease in permeability above 6 m, even though the residence time is increasing.

Not all changes in residence time are displayed in the analyzed microstructural parameters, especially at greater depths. Additionally the anisotropy and the air permeability of the firn clearly behave differently with regard to the residence time (Fig. 4a and b). Accordingly, other processes contribute to the evolution of firn properties with depth; the mechanisms for the genesis of anisotropy and permeability differ at depths below several meters in firn. Courville (2007) observed a much larger impact of small changes in accumulation pattern on microstructure and permeability in regions of very low accumulation than in regions of high accumulation. This might be one explanation for the less pronounced influence of changes in accumulation rate in the deeper firn layers, where the correlated accumulation rate was higher than in the uppermost meter. On the other hand, Rick and Albert (2004) show that the growth of necks between the grains is the dominant mechanism for permeability reduction at depths between approximately 2 and 10 m, and that a warming of temperatures over time would also impact metamorphism at this depth. Thus, the top ~10 m of firn is subject to a number of effects that would be reflected in the permeability of buried layers, including trends in surface temperature and accumulation rates. The calculated residence time is an integrated measure over the uppermost 2.5 m. We do not know the residence time of individual layers (e.g whether a certain layer has spent a certain fraction of the time in the very uppermost centimeters and might therefore be exposed to large temperature gradients, or whether it monotonically became buried below 2.5 m depth). Anisotropy is probably mainly generated within the upper few centimeters below the surface, where temperature gradients are largest. Permeability, on the other hand, could be the result of longer-term processes such as the interaction of air ventilation and coarsening, which increase the pore size or pore connectivity when densification does not overrule the effect. This seems to be the case in the upper 2.5 m at this site. Thus more differentiated residence times for different depth intervals need to be investigated.

CONCLUSION

The highly layered polar firn reflects the occurrence of metamorphism of different snow types at large timescales and under constantly changing environmental conditions. At Hercules Dome, the maximum in our permeability measurements from this site is consistent with measurements at other sites (Albert and others, 2000; Albert and Shultz, 2002; Rick and Albert, 2004) showing a permeability maximum near ~2.5 m depth. Our first results from 3-D microtomography scan imaging of polar firn show that this is accompanied by general firn coarsening (increase in both grain size and interstitial pore space) in this region. Below that, other processes including grain growth, necking and compaction influence the metamorphism of the microstructure. The texture of the firn shows distinct anisotropy throughout the profile, which is a result of vertical temperature gradients and subsequent water-vapor gradients. Short-term changes in accumulation rate affect the residence time of certain firn layers in the uppermost meter of the firn column, where rapid metamorphism takes place and the largest temperature gradients occur. We found a clear signature of changing accumulation rate in the firn-anisotropy and air-permeability profiles in the firn below approximately 5 m depth. Our data confirm that even though the effects of changes are most pronounced in the near surface, they remain evident through time as the firn becomes buried, even at this high-accumulation site.

ACKNOWLEDGEMENTS

We thank the US ITASE field team 2002 for drilling the core, and D. Dixon from University of Maine for providing the accumulation rate data of the site. This work was funded in part by German Science Foundation (DFG) grant FR2527/1-1 and supported by the German Academic Exchange Division (DAAD) and funded in part by US National Science Foundation grants NSF-OPP 0538492 and NSF-OPP 0229527 to M. Albert. We also thank the two anonymous reviewers for helpful comments.

REFERENCES

Albert, M.R. and E. Shultz. 2002. Snow and firn properties and air–snow transport processes at Summit, Greenland. *Atmos. Environ.,* **36**(15–16), 2789–2797.

Albert, M.R., E.F. Shultz and F.E. Perron, Jr. 2000. Snow and firn permeability at Siple Dome, Antarctica. *Ann. Glaciol.,* **31**, 353–356.

Albert, M., C. Shuman, Z. Courville, R. Bauer, M. Fahnestock and T. Scambos. 2004. Extreme firn metamorphism: impact of decades of vapor transport on near-surface firn at a low-accumulation glazed site on the East Antarctic plateau. *Ann. Glaciol.,* **39**, 73–78.

Alley, R.B. 1987. Texture of polar firn for remote sensing. *Ann. Glaciol.,* **9**, 1–4.

Alley, R.B. 1988. Concerning the deposition and diagenesis of strata in polar firn. *J. Glaciol.,* **34**(118), 283–290.

Alley, R.B., J.F. Bolzan and I.M. Whillans. 1982. Polar firn densification and grain growth. *Ann. Glaciol.,* **3**, 7–11.

Armbrecht, J. and T. Sych. 2005. *MAVI – Modular algorithms for volume images*. Kaiserslautern, Fraunhofer Institut für Techno- und Wirtschaftsmathematik.

Colbeck, S.C. 1983. Theory of metamorphism of dry snow. *J. Geophys. Res.,* **88**(C9), 5475–5482.

Coléou, C., B. Lesaffre, J.B. Brzoska, W. Ludwig and E. Boller. 2001. Three-dimensional snow images by X-ray microtomography. *Ann. Glaciol.,* **32**, 75–81.

Courville, Z.R. 2007. Gas diffusivity and air permeability of the firn from cold polar sites. (PhD thesis, Dartmouth College.)

Courville, Z.R., M.R. Albert, M.A. Fahnestock, L.M. Cathles and C.A. Shuman. 2007. Impacts of an accumulation hiatus on the physical properties of firn at a low-accumulation polar site. *J. Geophys. Res.,* **112**(F2), F02030. (10.1029/2005JF000429.)

Davis, R.E., E.M. Arons and M.R. Albert. 1996. Metamorphism of polar firn: significance of microstructure in energy, mass and chemical species transfer. *In* Wolff, E.W. and R.C. Bales, *eds. Chemical exchange between the atmosphere and polar snow.* Berlin, etc., Springer-Verlag, 379–401. (NATO ASI Series I: Global Environmental Change 43.)

Flin, F., J.-B. Brzoska, B. Lesaffre, C. Coléou and R.A. Pieritz. 2004. Three-dimensional geometric measurements of snow microstructural evolution under isothermal conditions. *Ann. Glaciol.,* **38**, 39–44.

Freitag, J., S. Kipstuhl and S.H. Faria. 2008. The connectivity of crystallite agglomerates in low-density firn at Kohnen station, Dronning Maud Land, Antarctica. *Ann. Glaciol.,* **49**, 114–120.

Gow, A.J. 1965. On the accumulation and seasonal stratification of snow at the South Pole. *J. Glaciol.,* **5**(40), 467–477.

Gow, A.J. 1969. On the rates of growth of grains and crystals in South Polar firn. *J. Glaciol.,* **8**(53), 241–252.

Hörhold, M.W. 2006. Microstructure and air transport properties of polar firn. (MS thesis, University of Bremen.)

Jacobel, R., B.C. Welch, E. Steig and D. Schneider. 2005. Glaciological and climatic significance of Hercules Dome, Antarctica – an optimal site for deep ice core drilling. *J. Geophys. Res.,* **110**(F1), F01015. (10.1029/2004JF000188.)

Kaempfer, T.U. and M. Schneebeli. 2007. Observation of isothermal metamorphism of new snow and interpretation as a sintering process. *J. Geophys. Res.,* **112**(D24), D24101. (10.1029/2007JD009047.)

Kaempfer, T.U., M. Schneebeli and S.A. Sokratov. 2005. A microstructural approach to model heat transfer in snow. *Geophys. Res. Lett.,* **32**(21), L21503. (10.1029/2005GL023873.)

Ohser, J. and F. Mücklich 2000. *Statistical analysis of microstructures in materials science*. Chichester, Wiley.

Palais, J.M., I.M. Whillans and C. Bull. 1982. Snow stratigraphic studies at Dome C, East Antarctica: an investigation of depositional and diagenetic processes. *Ann. Glaciol.,* **3**, 239–242.

Pieritz, R.A., J.B. Brzoska, F. Flin, B. Lesaffre and C. Coléou. 2004. From snow X-ray microtomograph raw volume data to micromechanics modeling: first results. *Ann. Glaciol.,* **38**, 52–58.

Rick, U.K. and M.R. Albert. 2004. Microstructure and permeability in the near-surface firn near a potential US deep-drilling site in West Antarctica. *Ann. Glaciol.,* **39**, 62–66.

Schneebeli, M. and S.A. Sokratov. 2004. Tomography of temperature gradient metamorphism of snow and associated changes in heat conductivity. *Hydrol. Process.,* **18**(18), 3655–3665.

Shiraiwa, T., H. Shoji, T. Saito, K. Yokoyama and O. Watanabe. 1996. Structure and dielectric properties of surface snow along the traverse route from coast to Dome Fuji Station, Queen Maud Land, Antarctica. *Proc. NIPR Symp. Polar Meteorol. Glaciol.,* **10**, 1–12.

Watanabe, O. 1978. Distribution of surface features of snow cover in Mizuho Plateau. *Mem. Natl Inst. Polar Res.,* Special Issue 7, 154–181.

Yosida, Z. *and 6 others*. 1955. Physical studies on deposited snow. I. Thermal properties. *Contrib. Inst. Low Temp. Sci. Ser. A* 7, 19–74.

MS received 18 February 2008 and accepted in revised form 27 January 2009